

# Temporary trapping of a light atom in between two heavy atoms

By EDVARDAS NAREVICIUS and NIMROD MOISEYEV

Department of Chemistry and Minerva Center of Nonlinear Physics in Complex Systems, Technion—Israel Institute of Technology, Haifa 32000, Israel

(Received 18 November 1997; accepted 14 March 1998)

The temporary trapping of a light atom in between two heavy atoms is associated with short lived overlapping resonances. It is shown for the electronically excited ArHCl that these quantum diffraction resonances can be associated, within the framework of the adiabatic approximation, with the non-physical poles of the scattering matrix when the light atom is scattered through one-dimensional dynamical barriers.

## 1. Are the overlapping poles of the scattering matrix observable?

For the one-dimensional (1D) and one channel problem the scattering matrix elements are defined as the ratio between the amplitude of the outgoing waves and the amplitude of the incoming waves. Therefore it is clear that the poles of the S-matrix can be obtained for specific values of  $E$  (real or complex eigenvalues of the Hamiltonian) either when the amplitude of the incoming wave-particle vanishes (i.e. physical poles), or when the amplitude of the outgoing wave has a pole [1] (i.e. false poles).

When the width,  $\Gamma_\alpha$ , of the pole,  $E_\alpha - (i/2)\Gamma_\alpha$ , is large enough then due to limitation of the number of significant figures in our computer (e.g.  $\exp(-N) = 0$ , when  $N > 400$ ), after a short time, which may be smaller than a single vibration in a molecule, the contribution of the broad poles to the propagation vanishes. It may happen that due to this technical difficulty the term  $\exp(-\Gamma t/\hbar)$  will vanish at  $t > \hbar/(E_{\alpha+1} - E_\alpha)$ , which is about the minimal time which is required to resolve the spectrum. However, even very broad poles which are associated with short lived metastable states (i.e. resonances) are not just a mathematical basis to expand the propagator but are observable. For example, the scattering matrix of  $e + H_2$  has extremely broad poles. The fact that these broad poles are associated with extremely short-lived negative ions,  $H_2^-$ , can be used to accelerate the ion in a strong electric field and to get high kinetic energy hydrogen which is needed for fusion reactions. The resonant electron–molecule collisions result in a variety of physical effects such as dissociative attachment which represents a source of negative ions in discharges and plasma, with possible applications in plasma heating and electromagnetic propulsion for space vehicles. Experimental observation of sharp structures in the cross-section for the vibrational excitations

( $v = 0 \rightarrow 3, 4$ ) in  $H_2$  by electron impact in the  $^2\Sigma_u^+$  resonance region obtained by Allan [2] (and are totally absent in  $v = 0 \rightarrow 1$  and  $0 \rightarrow 2$  and in  $e + D_2$ ) confirmed theoretical predictions of Domcke and co-workers [3]. This effect is a manifestation of the phenomenon postulated earlier for a general-model case by Domcke and Cederbaum [4]. These observations cannot be explained by the reflection principle [5] and provide examples to a possible physical effect made by extremely broad resonances. These results also show that the fact that the fingerprints of broad and overlapping resonances do not show up in a specific experiment (e.g.  $e + H_2(v = 0) \rightarrow e + H_2(v = 0, 1)$ ) does not guarantee that it will not play a role in another type of experiment (e.g.  $e + H_2(v = 0) \rightarrow e + H_2(v = 3, 4)$ ). (Overlapping resonances are defined as the poles of the S-matrix,  $E_\alpha - (i/2)\Gamma_\alpha$ , for which  $\Gamma_\alpha > |E_{\alpha\pm 1} - E_\alpha|$ ). Broad resonances can be considered as metastable states with  $\Gamma$  of the order of magnitude of the characteristic frequency of the system under study.)

Unlike the electron-scattering experiments where short lived resonances are seen and are very typical, such resonances are not seen in most cases for atom/molecular scattering experiments. The only known case to us where short lived resonances were measured in molecular beam scattering is the experiment of Neumark and co-workers [6]. Using electron photo-detachment spectroscopy (ZEKE technique) they measured directly the  $ClHCl^-$  resonances which have lifetimes of the order of 30–40 fs!

So far we have discussed the possibility of observing a single resonance. There may be cases, however, where the whole dynamics is controlled by a ‘pack’ of resonances. It may be hard to populate only a single resonance and to observe it. But the ‘pack’ of overlapping resonances dominates the dynamics. For example see the structured photoabsorption spectra obtained for

ArHCl when the initial state is a structureless Gaussian wavepacket [7] Another example is the HI molecule in a large Xe cluster. There is a large number of resonances representing the H atom inside the cage. No single resonance may be seen, but the resonances dominate the dynamics [8]

It is a common belief that it is impossible to separate out the energy variation of the resonance contribution to the scattering amplitude,  $T_{\text{res}}$ , when the resonances are overlapping resonances (the difference in their positions is much smaller than their widths).

The resonance scattering amplitude is given by

$$T_{\text{res}}(E) \propto \sum_{\alpha} \frac{C_{\alpha}}{E - E_{\alpha} + (i/2)\Gamma_{\alpha}}, \quad (1)$$

where the width of each Lorentzian peak obtained when  $|T_{\text{res}}|^2$  is plotted as function of  $E$  is  $\Gamma_{\alpha}$ .  
If,

$$|E_{\alpha+1} - E_{\alpha}| \ll \Gamma_{\alpha} \quad (2)$$

then  $|T_{\text{res}}(E)|^2$  will not show any structure as  $E$  is varied. However, except for rare cases as in the case of the poles of the S-matrix for the Eckart 1D potential, structure which is the fingerprint of the overlapping resonances 'pops out' when higher order derivatives of  $T_{\text{res}}(E)$  are taken,

$$\frac{\partial^n T_{\text{res}}(E)}{\partial E^n} \propto \sum_{\alpha} \frac{C_{\alpha}}{(E - E_{\alpha} + (i/2)\Gamma_{\alpha})^n}. \quad (3)$$

By now the Lorentzian peaks are about  $n/\ln 2$  times narrower than before. Similarly the structure which is the fingerprint of an individual resonance in a series of overlapping resonances might be seen as the high order derivative of the cross-section is taken.

From equation (3) one can get that if the overlapping resonances are such that  $E_{\alpha+1} - E_{\alpha} \approx \Gamma_{\alpha}/N$ , then their fingerprints will pop out by taking the  $2N$ th derivative of the energy-dependent photoabsorption spectra in half-collision experiments, and of the energy-dependent scattering cross-section in full collision experiments.

Another mechanism which can lead to the formation of a sharp structure in the scattering cross-section, although the resonances are broad and overlapping, has been discussed by Bohm [9]

Let us assume that  $E_1 = \varepsilon_1 - (i/2)\Gamma_1$  and  $E_2 = \varepsilon_2 - (i/2)\Gamma_2$  are two poles such that  $\Gamma_1 = \Gamma_2 = \Gamma$ ,  $\varepsilon_1 = 0$  and  $\varepsilon_2 = \Delta E$ . The cross-section in the neighbourhood of the poles is given by

$$\sigma(E) = \left| \frac{1}{E - \Delta E + (i/2)\Gamma} + \frac{C}{E + (i/2)\Gamma} \right|^2 \quad (4)$$

or

$$\sigma(E) = \sigma_1(E) + \sigma_2(E) + \sigma_{12}(E), \quad (5)$$

where  $\sigma_1(E)$  and  $\sigma_2(E)$  are the first and the second pole contributions to the cross-section:

$$\sigma_1(E) = \frac{1}{E^2 + \Gamma^2/4},$$

$$\sigma_2(E) = \frac{C^2}{(E - \Delta E)^2 + \Gamma^2/4}. \quad (7)$$

The last term in the equation (5),  $\sigma_{12}(E)$ , stands for the interference effect between the two poles:

$$\sigma_{12}(E) = \frac{2CE(E - \Delta E) + 2C\Gamma^2/4}{(E^2 + \Gamma^2/4)((E - \Delta E)^2 + \Gamma^2/4)}. \quad (7)$$

For  $C = -1$  and for  $\Delta E \leq \Gamma$  there is a single peak in the cross-section at  $E = \Delta E/2$ . However for  $C = 1$  and  $\Delta E = \Gamma$  the interference term  $\sigma_{12}(E = \Delta E/2)$  gives a zero contribution to the cross-section and consequently we obtain two well separated peaks in the cross-section. *As one can see the widths of the peaks in  $\sigma(E)$  are decreased due to the quantum interference effects.* Following the Heisenberg uncertainty principle the uncertainty in energy times the lifetime of the system is larger than  $\hbar/2$ . Therefore we may say that by narrowing the widths of the peaks in  $\sigma(E)$  one increases the lifetime of the system. Note that the usual concept of the lifetime as the inverse of the decay rate is applicable only for isolated resonances and not in our case where there is a large overlap between the different resonances.

## 2. The association of the 'non-physical' poles of 1D Eckart-type potential barriers with the resonances of three body system in two dimensions

Let us assume a three body system which consists of a light particle, A, and two heavy ones, B and C, which are held fixed at a distance  $R$  from one another. The interaction potential is taken here to be a short range repulsive one. This is a possible situation when A is a hydrogen atom and B and C are heavy Ar and Cl atoms when ArHCl is in the first excited electronic state (for which the Born–Oppenheimer potential curve is a repulsive one). For the sake of clarity and simplicity we first consider an interaction potential as a Heaviside step function. The B and C atoms are described as two discs with the same radius,  $r$ . The light particle A moves freely in the plane outside of the two discs (see figure 1).

Classically the light particle, A, can be trapped in between the two heavy atoms along the  $z$  axis. At a given energy there is only one principal periodic classical trajectory which is unstable. Therefore, an ensemble of non-interacting light particles centred at the unstable periodic orbit will spread in the two-dimensional (2D)

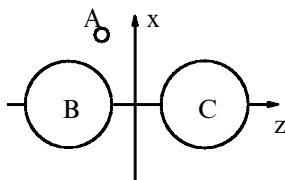


Figure 1. Illustrative picture of the studied model systems where the B and C heavy atoms are described as two discs and the light particle, A, moves freely in the plane, excluding the two discs area; i.e.  $V = \infty$ , when  $x^2 + (z \pm R/2)^2 \leq r^2$  where  $x, z$  denotes the coordinates of A.

space with a rate,  $k$ , where  $\exp(kt)$  is proportional to the averaged distance between the particles as a function of time. However, this is not a chaotic motion since there is only one unstable periodic orbit and this is not enough to produce chaos. A classical, so-called scattering chaotic motion is obtained when there are more than two heavy atoms. For the classical chaotic dynamics of such systems see, for example, the work of Gaspard and Rice [10]

The ArHCl potential energy surface which was taken from [11] shows that in the electronically excited ArHCl hydrogen moves almost freely in between the two heavy Ar and Cl atoms. Therefore, A in figure 1 can be regarded as hydrogen whereas B and C are regarded as chlorine and argon atoms.

On the basis of the classical dynamics of heavy-light-heavy particles, as described above we expect to have in quantum mechanics quasi-bound states which are associated with the unstable periodic orbits. All the poles of the S-matrix are expected to have about the same width (i.e. imaginary part of the complex pole) since they are all associated with the same unstable periodic orbit. Indeed, our 2D numerically exact quantum calculations (using the PES given in [11]) confirm this expectation.

All ArHCl poles which are presented in the first row of figure 2 have about the same width and are separated by the same quanta. Therefore they are associated with the unstable periodic orbit mentioned above. However, as one can see in figure 2 our results show that there are more (actually infinitely large number) of the poles which cannot be expected on the basis of classical calculations and are a consequence of the behaviour of the light hydrogen atom, A, acting as a wave and not as a classical particle. Later we will discuss this result in some more detail.

The poles which are presented in figure 2 are resonances which are associated with the temporary trapping of a hydrogen atom in between Ar and Cl. As we will discuss below only the first row of resonances in figure 2 have a classical analogue and are associated with the classical unstable periodic orbits. All other resonances

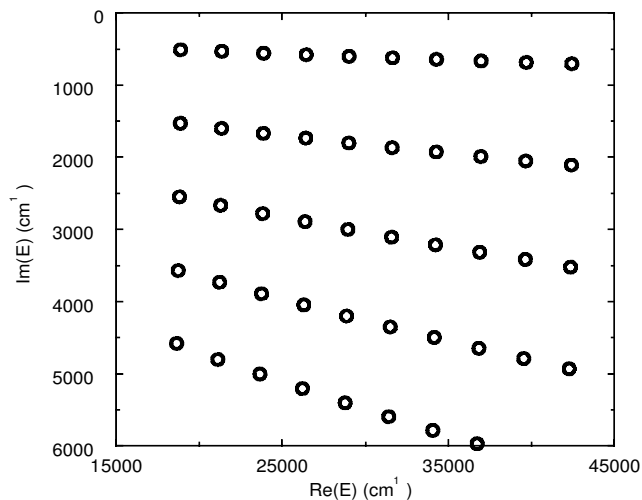


Figure 2. The numerically exact poles of the S-matrix as obtained from the quantum calculations by calculating the eigenvalues of the complex scaled ArHCl 2D Hamiltonian (i.e.  $x \rightarrow x \exp(i\theta)$ ) which are stable to small variations in  $\theta$ . The Ar-Cl distance was kept fixed at the equilibrium distance.

are quantum diffraction resonances which do not have a classical analogue.

For the sake of simplicity let us discuss their nature within the hard-sphere (or disc in two dimensions) approximation (although the calculations were carried out for the physical ArHCl potential). The bound states of the 1D potential,  $V(z; x)$  and  $-r \leq x \leq r$  ( $r$  is the radius of the discs representing the Ar and Cl atoms), are embedded in the continuum states which are associated with the  $V(z; x)$  potentials where the adiabatic coordinate  $x$  is taken as  $x > r$  or  $x < -r$ . Due to the non-adiabatic coupling potential terms the adiabatic bound states become metastable states. As one can see from the contours of the eigenfunctions of the complex-scaled Hamiltonian drawn in figures 3 and 4 they are localized in the  $\{x, z\}$  plane in between Ar and Cl (see figure 1) which is the classically accessible region in phase space.

The resonances shown in figure 3 are associated with the unstable periodic orbit since they are localized along it. Consequently these resonances have a classical analogue. The resonances shown in figure 4 are quantum diffraction resonances which are associated with the surface-wave dynamics that were well described by Connor [12] Quantum diffraction effects in this system, not necessarily of resonance character, were discussed by Gerber and co-workers [13] Although these resonances do not have a classical analogue they are localized in a classically accessible region in the phase space. By looking at the resonances in figure 4 we see that the complex scaled resonance wavefunction has one node

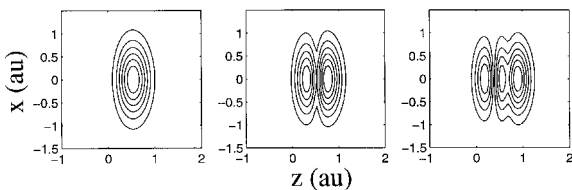


Figure 3. Contour plots of three eigenfunctions of the complex scaled ArHCl Hamiltonian which are associated with the unstable periodic orbit. These are the three first poles from the left, at the *first* row of poles presented in figure 2.

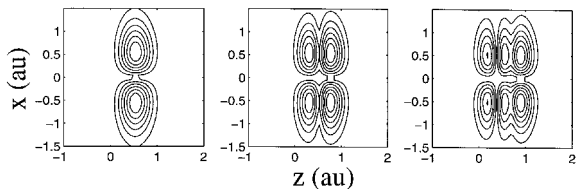


Figure 4. Contour plots of three eigenfunctions of the complex scaled ArHCl Hamiltonian which do not have a classical analogue. Here the three poles (counted from the left) are presented, which are shown at the second row of poles in figure 2.

along  $x$ . Therefore these resonances seem to be associated with oscillatory behaviour parallel to the  $z$  axis, i.e. above and below the Ar–Cl molecular axis. The transitions from the oscillations above the  $z$  axis to the oscillations below the  $z$  axis are due to the surface waves dynamics. See the illustrative picture given in figure 5.

We will show now that the 2D shape-type resonances described above are associated with the 1D poles of an Eckart-type potential. Within the framework of the adiabatic approximation the 1D shape type non-physical resonances are approximations to the physical 2D resonances.

Usually the adiabatic approximation is taken, as in the Born–Oppenheimer approximation, when one particle is much heavier than the other one. We will use here an unusual adiabatic approach. Here we will treat  $x$  as the adiabatic coordinate since the motion of hydrogen along  $x$  should be much slower than the motion along

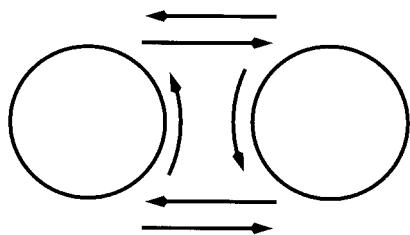


Figure 5. Illustrative picture of the diffraction resonance due to the ‘gliding’ of surface waves on the edge of the two discs that represent the heavy atoms.

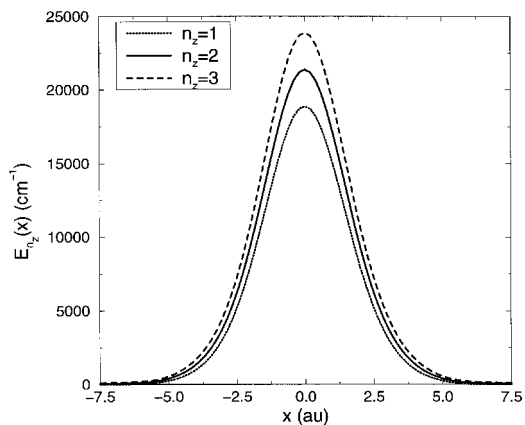


Figure 6. The adiabatic potentials,  $E_{n_z}(x)$ , obtained when the  $x$  coordinate in figure 5 has been treated as a parameter. The adiabatic potentials presented here look like Eckart potential barriers even with enlargement by high scaling factors.

the  $z$  axis in order to get a temporary trapping of the light ‘particle’ in between the two heavy atoms (represented as B and C in figure 1). Let us first consider the model where the two heavy atoms are described as two discs with the same radius  $r$  and hydrogen atom moving freely in the plane, excluding the area of the two discs. When  $x$  is treated as a parameter we reduce the problem from a 2D to 1D particle-in-a-box problem with a box length  $L(x) = R - 2(r^2 - x^2)^{1/2}$ , when  $-r \leq x \leq +r$ , and  $L = \mathcal{L}$  elsewhere.  $\mathcal{L}$  is the length of the artificial box which has been used in the numerical calculations. The adiabatic potentials are,  $E_{n_z}(x) = (\hbar \pi n_z / L(x))^2 / (2m)$ ;  $n_z = 1, 2, \dots$ . In figure 6 we represent the adiabatic potentials  $E_{n_z}(x)$  obtained from our numerical calculations for the *physical* ArHCl potential (soft repulsive potential) and not for the hard-disc/sphere pictures used above to clarify the trapping phenomenon of hydrogen in between two heavy atoms in the absence of attractive force. The shape of the adiabatic 1D potentials, obtained in our numerical calculation is very close to the Eckart potential barriers (i.e. inverse of square of the cosh function). The coalescence between these two types of potentials is remarkable even on large scale plots.

In the last step of the adiabatic calculations we calculated the  $n_x = 0, 1, 2, \dots$  complex eigenvalues of the complex scaled Hamiltonian,

$$H_{\theta}(x; n_z) = - \exp(-2i\theta) \frac{\hbar^2}{2m} \frac{d^2}{dx^2} + E_{n_z}(x \exp(+i\theta))$$

using the Collbert–Miller discrete-variable-representation expressions [14]. It is clear from the equation given above that within the framework of the adiabatic approximation the complex poles can be assigned by

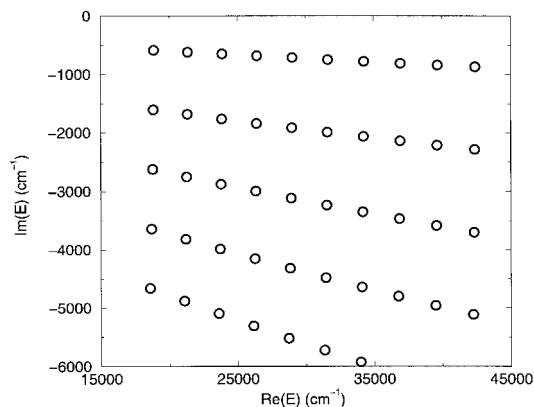


Figure 7. The poles of the 1D Eckart-type potentials represented in figure 1 as obtained by calculating the  $\theta$  independent eigenvalues of the complex-scaled ArHCl adiabatic Hamiltonians,  $H_\theta(x; n_z)$ ,  $n_z = 1, 2, \dots, 10$ . Notice the remarkable agreement with the numerical exact results presented in figure 6.

two good quantum numbers,  $n_x, n_z$ . The poles of the 1D Eckart-type potential barriers,  $E_{n_z}(x)$ , are given in figure 7. They are in remarkable agreement with the numerical exact results presented in figure 2. Beside the physical insight we get by the use of the adiabatic approach we also gain in the drastic reduction of the computational effort which is required for calculating the poles. Since the number of operations for calculating the  $N$  eigenvalues of a  $N \times N$  matrix is scaled as  $N^3$ , we reduce the length of the calculations by 6 orders of magnitude by using the adiabatic approach ( $N = 100$  has been taken as a representative number of basis functions for the  $z$  coordinate).

Here we have shown that the non-resonance poles of 1D Eckart-type potential barrier (associated with complex scaled eigenfunctions which are localized in the forbidden classical region in 2D phase space) are the resonance poles of the 2D problem and are associated with complex-scaled eigenfunctions which are localized in the classically accessible region in the four-dimensional phase space.

### 3. The disappearance of resonances in the transition from two to three dimensions: the effect of the quantum uncertainty principle

In three dimensions three atoms move in a plane when the total angular momentum  $J=0$ . Can we choose a specific plane such as  $y=0$ ? The motivation is clear. The calculations in two dimensions are faster by several orders of magnitude than the calculations in three dimensions. It is a common assumption that the basic dynamical properties of the system will be obtained from the 2D calculations although resonance effects

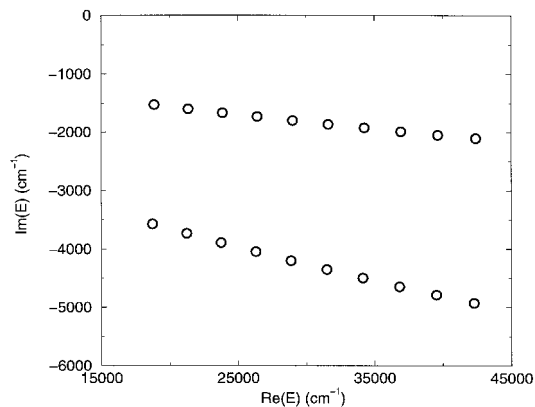


Figure 8. The resonance poles of the S-matrix as obtained by the complex coordinate method for the 3D ArHCl Hamiltonian.

will be more pronounced in the 2D dynamical studies. As we will explain below this assumption may hold only when the frequency of the bending mode of ABC is very high. For soft bending modes or for imaginary frequency bending modes, as discussed in this work, this assumption cannot be justified. For example we will show that the ArHCl 2D resonances which are associated with the classical unstable periodic orbits do not exist in three-dimensional (3D) space. In figure 8 we represent the poles for a model of a light particle, A (hydrogen), which collides with two heavy B, C (chlorine and argon atoms) ‘spheres’, rather than ‘discs’. Note again that the use of the discs/spheres terminology is used only in the analysis of the dynamics but the soft physical ArHCl 3D potential has been used in our calculations. The results we will present below were obtained from the 3D calculations where we used the cylindrical coordinates and ignored the  $-\hbar^2/8m\rho^2$  kinetic energy term in order to illustrate the elimination of 2D resonances that have a classical analogue. The inclusion of the  $-\hbar^2/8m\rho^2$  kinetic energy term in the 3D calculations shifts ‘down’ the resonance widths by about  $500\text{cm}^{-1}$  and does not change the resonance structure (i.e. rows of poles with about the same values for the width). The motion is in a plane since the angular momentum quantum number in the cylindrical coordinate representation of the Hamiltonian is taken to be equal to zero. A comparison of figure 8 with the results obtained in the 2D calculations, figures 2 and 7, shows clearly that *only* every other row of resonances obtained in the 2D calculations appears also in the 3D calculations. The 2D resonances associated with the  $n_x = 0, 2, 4, \dots, 2n, \dots$  do *not* exist in the 3D ‘world’. Since only the  $n_x = 0$  resonances (the resonances in the first row in figures 2 and 7) are associated with the classical unstable orbits it is clear that in three dimen-

sions there are only diffraction resonances with zero probability along the Ar–Cl molecular axis which is the  $z$  axis in our notation. The 2D calculations not only give the wrong impression that the resonances are sufficiently narrow to be considered as isolated resonances (in three dimensions the resonances are broader by a factor of 3–4 and are overlapping resonances) but also make the wrong impression that there is a classical analogue to the resonance phenomenon in this problem. Note, however, that since the resonance widths vanish in the limit of  $\hbar \rightarrow 0$  the ArHCl resonances are not considered as Feshbach-type resonances. In this sense all the ArHCl resonances in the 3D/2D ‘world’, including the diffraction resonances which do not have a simple classical analogue, are shape-type resonances which are associated with a dynamical potential energy barrier.

There are several ways to explain the disappearance of every other set of resonances in the transition from the 2D to the 3D ‘world’. We will give here three explanations. The last one will be more formal than the first two explanations.

(1) The quantum uncertainty principle does not allow us to determine a plane or a line in the 3D ‘world’. A  $\{x, z\}$  plane at  $y = 0$  implies that we know not only the  $y$  position of the atoms but also their  $y$  component of momentum since they do not leave this plane and therefore  $p_y = 0$ . From the same arguments it is clear that collinear molecules do not exist. When we say for example that  $\text{CO}_2$  is a collinear molecule we still accept the fact that there is a bending motion even in the ground electronic, vibrational and rotational state of  $\text{CO}_2$ . Therefore,  $\text{CO}_2$  is not a linear molecule in the mathematical sense. However for  $\text{CO}_2$  the frequency of the bending motion reaches a sufficiently high value to cause the  $\text{CO}_2$  molecule to have a structure which is very close to a linear shape. In our case the bending modes do not exist at all and the bending mode frequency is imaginary and close to zero. Therefore the motion of hydrogen along the  $x$  and  $y$  coordinates is almost a free motion. Hydrogen will never ‘bounce-back’ whenever it gets out of the  $(x = 0, y = 0, z)$  line.

(2) Since we know that the dynamics of three atoms with a zero total angular momentum is in a plane, let us choose a specific plane  $\{u, z\}$  which includes the  $z$  axis (i.e. the Ar–Cl molecular axis). The plane will be uniquely defined by the rotational angle  $\alpha$  when  $u = \cos(\alpha)x + \sin(\alpha)y$ . The solutions of the 2D time independent Schrödinger equation,  $\tilde{\chi}(u(\alpha), z)$ , are functions of  $u(\alpha)$  and  $z$ . At  $u(\alpha) = 0$  all solutions depend on  $z$  only. The solutions obtained for different values of  $\alpha$  are identical up to a random phase factor when  $u = 0$ . That is  $\chi(u = 0, z) = \tilde{\chi}(u(\alpha) = 0, z) \exp[i\gamma(\alpha)]$ ;  $0 \leq \gamma(\alpha) \leq 2\pi$ , are the solutions obtained for different

choices of the plane  $\{z, u\}$ . The cumulative random phase factor is zero. That is  $\int_0^{2\pi} \exp[i\gamma(\alpha)] d\alpha = 0$  if  $f(\alpha)$  varies randomly with  $\alpha$ . Therefore the solutions obtained in the 3D calculation,  $\chi(x, y, z) = 1/2\pi \int_0^{2\pi} \chi(u(\alpha), z) d\alpha$  have zero value for any value of  $z$  when  $x = 0$  and  $y = 0$  (i.e. when  $u(\alpha) = 0$ ). This result makes it impossible to obtain in three dimensions the resonances which were obtained in the 2D calculations and have maximal amplitude at  $x = y = 0$  (see figure 3). The only 2D resonances which ‘survive’ in the 3D space are those which have a zero amplitude along the line  $u = 0$ , i.e.  $x = 0$  in our choice of coordinates, in the 2D numerical calculations (see figure 4).

(3) When the cylindrical coordinates are used to describe the three-body problem in 3D space the volume element is given by  $d\tau = \rho d\rho d\phi dz$ . The probability of finding the atoms in a given orientation is the *density probability* (i.e. the square of the absolute value of the eigenfunction) times the volume element,  $d\tau$ . Since  $d\tau = 0$  when  $\rho = 0$  it is clear that the probability of finding the 3 atoms at  $\rho = 0$  is zero.

Another way to see why the probability to find hydrogen at  $\rho = 0$  is zero, is by carrying out the following transformation:

$$\Psi(\rho, z, \phi) = \chi(\rho, z, \phi) \rho^{-1/2}. \quad (8)$$

The normalization condition for the  $\Psi(\rho, z, \phi)$  is determined by the integral  $\int |\Psi|^2 \rho d\rho dz d\phi$ , and therefore that for the function  $\chi(\rho, z, \phi)$  is determined by the integral  $\int |\chi|^2 d\rho dz d\phi$ . Since the potential is finite everywhere, the wavefunction  $\Psi$  must also be finite in all space, including the origin. Hence it follows that  $\chi(\rho, z, \phi)$  must vanish for  $\rho = 0$ ,

$$\chi(\rho = 0, z, \phi) = 0. \quad (9)$$

Here we follow a very similar derivation given in Landau and Lifshitz book (see equation (32.11) in [15]) for a centrally symmetric potential and where the spherical rather than cylindrical coordinates are employed.

From equation (9) one can see that the maximal probability to find the 3 atoms  $|\chi(\rho, z, \phi)|^2$  is at  $\rho \neq 0$ . For very similar reasons the s-type orbitals are plotted in text books as spheres with a radius which can never be equal to zero. Since  $\rho = (x^2 + y^2)^{1/2}$  it implies that the resonance solutions in two dimensions which get maximal value at  $x = y = 0$  should be excluded in the transition to 3D space.

#### 4. Concluding remarks

The temporary trapping of hydrogen in between Ar and Cl has been associated with resonances calculated by the complex coordinate method. All of them are localized in the classically accessible region in the coor-

dinate-momentum space. Therefore they are accessible in scattering experiments. The resonances produce a crystal-like structure in the complex energy plane (figures 2, 7 and 8). The first row of the resonances which are obtained in the 2D calculations and have about the same width are associated with the classical unstable periodic orbits (figures 2 and 7). All other resonances are quantum diffraction resonances. Their nature and their structure are resolved by using the adiabatic approximation where the motion of hydrogen along the coordinate which is perpendicular to the Ar and Cl axis is treated as the slow coordinate. Within the framework of the adiabatic approximation the dynamical barrier is exposed and the resonances are obtained by calculating the poles of 1D Eckart-type potential barriers. The poles are localized (upon complex scaling) in the classical forbidden 1D phase space. Therefore in 1D scattering experiments these poles are not physical and do not have any physical observable effects. The dynamics, however, are not in 1D space and therefore these poles are accessible. In three dimensions due to the quantum uncertainty principle only every other 2D resonance survives. Therefore, in 3D space there is no trapping of hydrogen in resonance states which are associated with the classically unstable periodic orbits. All hydrogen trappings are quantum phenomena associated with the diffraction resonance states.

We thank Professor W. H. Miller for most enlightening discussions about resonances and poles during his stay at the Technion as a distinguished Israel Pollak

invited professor. Professors Wolfgang Domcke, Benny Gerber and Jürgen Korsch are acknowledged for most helpful discussions and comments.

### References

- [1] TAYLOR, J. R., 1972, *Scattering Theory: The Quantum Theory of Non-relativistic Collisions* (New York: John Wiley and Sons, Inc.).
- [2] ALLAN, M., 1985, *J. Phys. B*, **18**, L451.
- [3] MUNDEL, C., BERMAN, M., and DOMCKE, W., 1985, *Phys. Rev. A*, **32**, 181; GERTTSHKE, PI. I., and DOMCKE, W., 1993, *Phys. Rev. A*, **47**, 1031.
- [4] DOMCKE, W., and CEDERBAUM, L. S., 1980, *J. Phys. B*, **13**, 2829.
- [5] SCHINKE, R., 1993, *Photodissociation Dynamics* (Cambridge: Cambridge University Press), pp. 316–319.
- [6] METZ, R. B., KITSOPOULOS, T. N., BRADFORTH, S. E., and NEUMARK, D. N., 1988, *J. phys. Chem.*, **92**, 5558.
- [7] NAREVICIUS, E., and MOISEYEV, N., 1998, *Chem. Phys. Lett.*, **287**, 250.
- [8] ALIMI, R., and GERBER, R. B., 1990, *Phys. Rev. Lett.*, **64**, 1453.
- [9] BOHM, A., 1986, *Quantum Mechanics: Foundations and Applications* (New York: Springer-Verlag).
- [10] GASPARD, P., and RICE, S. A. 1989, *J. chem. Phys.*, **90**, 2225; 1989, *ibid.*, 2242; 1989, *ibid.*, 2255.
- [11] GARCIA-VELA, A., GERBER, R. B., and VALENTINI, J. J., 1991, *Chem. Phys. Lett.*, **186**, 223.
- [12] CONNOR, J. N. L., 1990, *J. chem. Soc. Faraday Trans.*, **86**, 1627.
- [13] GARCIA-VELA, A., GERBER, R. B., and IMRE, D. G., 1992, *J. chem. Phys.*, **97**, 7242.
- [14] COLBERT, D. T., and MILLER, W. H., 1992, *J. chem. Phys.*, **96**, 1982.
- [15] LANDAU, L. D., and LIFSHITZ, E. M., 1965, *Quantum Mechanics* (Oxford: Pergamon).